Investigation on the Effect of Electron and Hole Doping on Electronic Structure and Superconductivity in MgB_2

Vaishali Yadav[1], Rimpy Shukla[1], Ritu Sharma[2], Krishna S. Sharma[1]*
[1]Department of Physics, The IIS University, Jaipur
[2]Department of Electronics, Malviya National Institute of Technology, Jaipur

Abstract

In this paper the effect of electron doping (through partial replacement of B by C) and hole doping (through partial replacement of B by Be) on electronic structure of MgB_2 has been investigated by using WIEN2K code, based on Density Functional Theory. Perdew-Burke-Ernzerhof (96) pseudo-potential is used for solving the Schrödinger equation in self-consistent manner and the exchange and correlation effects are accounted for through the use of Generalized Gradient Approximation. The band structure and density of states obtained from the above mentioned pseudo-potential for the doped MgB_2 with doping levels of 25% and 50% of C and Be, are found to provide satisfactory explanation to the experimentally observed superconducting behaviour of this material both for electron and hole doping. The Dirac point like structure obtained in the band structure of MgB_2 at symmetry point K, when used with hole filling of $p_{x,y}$ (σ) bands in $\Gamma - A$ direction and Density of States at Fermi level, is found to be quite useful in explaining the effect of electron/hole doping on superconductivity in MgB_2.

Introduction

Since the discovery of superconductivity in MgB_2 with transition temperature (T_c) of the order of 40K in 2001 by Nagamatsu *et al.* (2001), much activity has taken place in scientific community. A large number of researches, both experimental and theoretical, were reported soon after its discovery on superconducting and other properties of MgB_2 and other related materials. MgB_2 has a planer structure in which boron atoms form a honeycomb lattice and hexagonal layers of Mg atoms act as fillers in between two boron layers, such that an Mg atom lies just above the centre of a hexagon in boron layer. The origin of T_c of the order of 40 K in MgB_2, higher than other conventional superconductors, has been a matter of concern for theoretical researchers. Kortus *et al.* (2001) observed that MgB_2 is essentially the metallic boron, held together by means of strong covalent B-B in-plane bonding and weak ionic B-Mg out of the plane bonding. It is electronically a typical sp metal, with a typical Density of States (DOS) at Fermi level. Strong bonding and high frequency vibrations in boron plane result in strong electron-ion scattering and strong electron-phonon coupling. According to them, the fortunate combination of strong bonding, reasonable density of states at the Fermi level and higher values of phonon frequencies, give rise to strong electron-phonon coupling, which may be considered responsible for the higher values of T_c in this compound. Kong *et al.* (2001)

concluded that the unexpectedly high value of T_c in MgB_2 may be considered to arise as a result of the large value of electron-phonon coupling strength (λ), which in turn may be attributed to the presence of holes in the B-B bonding σ-bands and bond stretching due to optical phonon vibrational modes. Ravindran *et al.* (2001) identified a doubly degenerate quasi-two dimensional energy band in the vicinity of the Fermi level, along the Γ-A direction of Brillöuin zone, which along with non-zero Density of States at the Fermi level, 2D structure of honeycomb B-layers in MgB_2 and large anisotropy of phonon modes may be considered to be responsible for the observed superconductivity in MgB_2. They also investigated isoelectronic compounds, like BeB_2, CaB_2, SrB_2, LiBC and MgB_2C_2 and found that the hole doped LiBC and MgB_2C_2 may be considered as the potential superconducting materials. Okatov *et al.* (2001) observed that quasi-2D bands in MgB_2 are obtained from dispersion E(k) of B $2p_{x,y}$ like bands in the $k_{x,y}$ (Γ-K) direction. They form a flat zone in k_z (Γ-A) direction and reflect the distribution of pp_σ states in the boron layers. These states make considerable contribution to DOS at Fermi level, resulting in metallic properties of diborides. The 3D type of bands originating from weaker pp_π interactions due to B $2p_z$-like bands, show maximum dispersion in the k_z (Γ-A) direction. According to them, the peculiar electronic properties of MgB_2 can be associated with the metal like 2p states of

boron atom layers, which also determine the DOS distribution in the vicinity of Fermi level. Similar observations were also made by Mater (2008), Milman and Warren (2001) and Fan *et al.* (2002) regarding the electronic behaviour of MgB_2 and other related compounds.

Investigations made by Sharma *et al.* (2010) in BCS-Eliashberg framework by employing Mc-Millan's T_c-equation (Mc-Millan, 1968) reveal that the phonon mediated e-e interaction, coupled with higher values of phonon frequencies due to vibrational modes of light mass B-atoms, particularly in the plane of boron layers, give rise to higher values (of the order of 1) electron-phonon coupling strength (λ), which may be considered responsible for the superconducting phase transition of MgB_2 at comparatively higher values of T_c. The conditions are not that favourable in other metallic oxides, like AlB_2, BeB_2, CaB_2, NbB_2 etc., which either do not become superconductor or show superconductivity at much lower values of T_c, as compared to MgB_2 (Ravindran *et al.*, 2001; Goyal *et al.*, 2012 ; Medvedeva *et al.*, 2001). Medvedeva *et al.* (2001) used full potential linear muffin-tin potential in Generalized Gradient Approximation (GGA) for electronic structure calculations of MgB_2 and other metallic diborides. They observed that superconductivity in these compounds is related to the existence of $p_{x,y}$-band holes at Γ point. On that basis, they were able to explain the experimentally observed superconducting features of MgB_2 and other metallic diborides like, BeB_2, AlB_2, ScB_2 and YB_2. They also predicted possibility of medium-T_c superconductivity in CaB_2 with T_c values higher than that of MgB_2 through a similar treatment, though it could not be experimentally verified so far.

According to Liu *et al.* (2001), the E_{2g} phonons in MgB_2, which involve in-plane B displacements along Γ- A line, couple strongly with the $p_{x,y}$ electron bands. They noticed presence of multiple gaps in the band structure of MgB_2 and by using two-phonon scattering, observed that the E_{2g} phonons are strongly anharmonic and the nonlinear contribution to the coupling between E_{2g} modes and the $p_{x,y}$ bands is significant. They obtained effective value of electron-phonon coupling constant to be $\lambda \approx 1.01$. An and Pickett (2001) observed that MgB_2 can be characterized by its ionic form $Mg^{2+}(B_2)^{2-}$. The attractive potential of Mg^{2+} between B_2 layers lowers the π bands, resulting in $\sigma \rightarrow \pi$ charge transfer that derives the hole doping of the s bands. The σ bands are strongly 2D, the dispersion along Γ- A direction being very little. The E_{2g} phonon modes break the symmetry and split the σ bands by about 1.5 eV along Γ- A line. They further observed that coupling of the σ bands to the bond stretching phonon modes may provide most of the coupling to account for the observed values of T_c.

Choi *et al.* (2002) proposed two band model to explain superconductivity in MgB_2. According to them the strong coupling results in strong electron pair formation of σ-bonding states of boron $p_{x,y}$ orbitals, confined to the boron planes, which give rise to an average energy gap of $\Delta_1 \approx 6.8$ meV and correspond to two cylindrical sheets of the Fermi surface around Γ- A line, bulging out at the centre. The π-bonding states of boron p_z orbitals, which correspond to the remaining two sheets of Fermi surface, form much weaker pairs with average energy gap $\Delta_2 \approx 1.8$ meV. These energy gaps are temperature dependent and become zero as $T \rightarrow T_c$. The size of the gap also changes on different sections of the Fermi surface. According to them, the σ-bonding states and inter band scattering contribute to higher T_c superconductivity in MgB_2. It may, therefore, be concluded that the origin of higher value of T_c in MgB_2 lies in its electronic structure. As such, the electronic structure studies of MgB_2 and related materials are important, as the same can be correlated with their T_c values.

The present authors noticed that in addition to the above, the presence of a Dirac point like structure in the energy band diagram of MgB_2 at symmetry point K, similar to that obtained in the energy band diagram of graphene (Sharma *et al.*, 2017), is also an important feature of the electronic band structure of MgB_2, which may be used to explain superconductivity in MgB_2 and related materials. But there is one important difference between them. In graphene it is obtained at the Fermi level, whereas in MgB_2 it appears about 2.0 eV above the Fermi level, as apparent from the band structure diagrams for this material reported by Medvedeva *et al.* (2001), Ruiz-Chavarria *et al.* (2006) and Pena *et al.* (2002). At the Dirac point the E-K diagram is linear and electrons behave as mass-less particles, which may facilitate their pairing and correlated motion. Thus, the presence of Dirac electrons at K point and filling of holes in the valence band in Γ-A direction, along with moderate values of density of states at the Fermi level and strong coupling of high frequency phonon modes of boron lattice with $p_{x,y}$ (σ) bands may be considered to be responsible for creating favourable conditions in MgB_2 for its phase transition to superconducting state at higher temperatures of the order of 40K. It may be observed from Medvedeva *et al.* (2001) that although in AlB_2 a Dirac point like structure exists at Fermi level, but the valence band in Γ-A region is well below the Fermi level. As such, there is no possibility of hole filling in the valence band, with the result that the conditions in AlB_2 are not favourable for it to become superconducting. On the other hand, for BeB_2 valence band in Γ-A region lies just above the Fermi level so that hole filling in it becomes possible, but the Dirac point like structure at K point is absent. The result is that in BeB_2 also, the conditions are not as favourable as in

IISU

MgB_2 for it to become superconductor. In CaB_2, the Density of States at Fermi level (≈ 0.92 states/eV) is found to be more than that of MgB_2 (≈ 0.73 states/eV) and the valence band in Γ-A region lies just above the Fermi level so that hole filling in this band becomes possible. It may also be observed from Medvedeva *et al.* (2001) that for CaB_2 the Dirac point like structure is obtained at the Fermi level, showing that favourable conditions exist for it to become superconductor at higher values of T_c, but it is an experimentally verified fact that CaB_2 is not stable. Other factors, such as larger values of lattice parameters and increased interlayer separation in CaB_2, as compared to MgB_2, may also affect the expected results.

It may be quite interesting to investigate the effect of electron/hole doping on the electronic structure and superconductivity of MgB_2. For example, since carbon has one more valence electron as compared to boron, substitution of a boron atom by carbon atom results in electron doping of MgB_2. A similar effect is created on substituting Mg atom by Al atom in MgB_2. On the other hand, since Be atom has one less valence electron than B, substitution of a B atom by Be atom results in hole doping of MgB_2. A similar effect can also be created on substituting Mg atom by Na atom in MgB_2. The density of electrons/holes in the doped MgB_2, however, depends on percentage of Mg or B atoms substituted by the impurity atoms.

For electron doping of MgB_2, several works have been reported on superconducting and other properties of carbon substituted MgB_2. Some of these works, which need to be mentioned here are Medvedeva *et al.* (2001), Bateni *et al.* (2015), Sunser *et al.* (2014), Gargee Sharma (2016), Kim and Choi (2015), Shaikh *et al.* (2013), Yeoh *et al.* (2011), Mudgel *et al.* (2009), Kazakov *et al.* (2005), Mickelson *et al.* (2002), Dai *et al.* (2011) and Prabhakar P. Singh (2003). Through substitution of B by C from 3% to 20%, Kazakov *et al.* (2005) observed that T_c of MgB_2 decreased from 38.5 to 10.2 K. Also the lattice parameter 'a' was found to decrease with increasing carbon percentage, whereas the lattice parameter 'c' was found to first increase and then decrease. Shaikh *et al.* (2013), on the other hand, observed by co-doping of MgB_2 with nano-Alumina and nano-carbon, that on doping with 2% Al, T_c of MgB_2 decreases from about 36 K to 28 K, which starts increasing on its carbon doping and may attain a value of the order of 37 K for 3% carbon. Experimental investigations made by Dai *et al.* (2011) on carbon doped MgB_2 thin films, show that both the lattice parameters (a and c) increase with carbon content in the thin films. It was found that T_c dropped slowly, and the residual resistivity increased considerably with increase in carbon doping. Medvedeva *et al.* (2001) also demonstrated that the electron doping of MgB_2 by substitution of B by C, N or O or creation of defects in B-sublattice are not favourable for superconductivity.

According to them, the hole doping or isoelectronic substitution of Mg by Ca, Na, Cu or Zn or substitution of B by Li or Be may give rise to a superconductor with similar or higher values of T_c, although the experimental verification of the same is not yet available. Prabhakar P. Singh (2003) has studied electronic structure and determined T_c values of $Mg(B_{1-x}C_x)_2$ for $0 \leq x \leq 0.3$. He observed that the changes in electronic structure of MgB_2 on its carbon doping, specially near the Fermi energy, come mainly from outward movement of E_F with increasing x, accompanied by a sharp decline in both B and $C_{px(y)}$ states for $0.2 \leq x \leq 0.3$. The calculations made by them show a decline in T_c with increase in x.

Chavarria *et al.* (2006) investigated the band structure of carbon doped MgB_2. It was shown that on doping MgB_2 with carbon, valence band goes down, so much so that for $x = 0.68$ the valence band for $MgB_{2-x}C_x$ in Γ-A direction is completely below the Fermi level and becomes full with electrons, so that there is no possibility of hole filling in the valence band. Also it may be observed from the band structure calculated by them that the Dirac point like structure at K point now goes below the Fermi level. These may be considered as the probable reasons for reduction in T_c of MgB_2 on doping it with carbon, T_c approaching 0 K for $x \approx 0.36$. On doping MgB_2 with Al, it was observed by them that in $Mg_{1-x}Al_xB_2$, T_c almost approaches 0K for $x \approx 0.56$, although in that case the Dirac point like structure at K point is found to lie just above the Fermi level. This shows that for favourable conditions for superconductivity to occur, the position of both the Dirac point like structure at K point and valence band in Γ-A direction are very critical, which should lie just above the Fermi level for superconductivity to occur. Kortus *et al.* (2005) also observed that the decrease in T_c on doping MgB_2 with Al or C can be explained in terms of band filling effect due to electron doping by Al or C. They observed that the dependence of T_c on electron doping can be explained in terms of dependence of electron-phonon coupling strength (λ) and density of states at Fermi level $N(E_F)$ on electron doping. They further observed that the reason for obtaining almost constant band gap for various levels of electron doping in MgB_2 lies in mutual compensation of the effects of band filling and inter-band scattering. They also observed that scattering by non-magnetic impurities should have a pair breaking effect, which along with the inter band scattering leads to a decrease in T_c.

Important works on Al doping of MgB_2 are due to Slusky *et al.* (2001), Shah *et al.* (2009), Lorentz *et al.* (2001) and Pena (2002). Slusky *et al.* (2001) reported that in $Mg_{1-x}Al_xB_2$, T_c drops smoothly up to $x = 0.1$, beyond which a two phase mixture of B-rich and Al-rich phases occurs. At $x = 0.25$ and beyond, a single phase non-superconducting

system is restored, i.e., filling of σ bands destroys superconductivity. According to the rigid band model, the filling of σ bands decreases T_c moderately initially, but as the σ bands become nearly full, the coupling decreases abruptly and T_c vanishes. Neaton and Perali (2001) investigated the effect of substitution of Mg by Ca, Na and Al in MgB_2. Whereas Ca is isoelectronic to Mg, Al substitution gives rise to electron doping and Na substitution produces hole doping in MgB_2. They found T_c to decrease almost linearly with increase in percentage of Al, but on increasing the percentage of Ca or Na in MgB_2, T_c was found to increase linearly. They attributed increase in T_c on substitution of Mg by Ca to increase in unit cell volume. For substitution of Mg by Na, the removal of an electron from the unit cell and increase in the unit cell volume were considered to be the possible reasons for increase in T_c. For Al doping of MgB_2, the addition of an electron in the unit cell and decrease in unit cell volume were considered to be responsible for decrease in T_c. Structure and superconducting state properties of Ca-doped MgB_2 superconductors were experimentally investigated by Sun *et al.* (2007), who observed that both the lattice parameters 'a' and 'c' of MgB_2 are enlarged on its Ca-doping and the transition temperature (T_c) is suppressed, its value changing from 37.8 K for pure MgB_2 to 36.5 K for $Mg_{0.92}Ca_{0.08}B_2$, which contradicts the theoretically predicted result of Neaton and Perali (2001), mentioned above.

Cai *et al.* (2014) have compared the superconducting properties of carbon doped MgB_2 bulk fabricated from pre-synthesized Mg/CNT and Mg/amorphous carbon composites. They found that the performance of critical current density (J_c) at high fields was improved for CNT-doped samples, whereas in amorphous C-doped samples, J_c performance was improved over the entire field range. The doping effect of carbon nano tubes (CNT) and nano-carbon (NC) in MgB_2 bulk was also studied by Lim *et al.* (2009). They observed higher T_c values for CNT-doped MgB_2 as compared to NC-doped samples. They also observed that J_c behaviour was improved both for CNT and NC doping.

Recent works on investigation of superconducting state properties of graphene doped MgB_2 are Sudesh *et al.* (2013), De Silva *et al.* (2011; 2012), Li *et al.* (2017) and Wu *et al.* (2016). All these authors report improvement in J_c performance and increase in H_{c2} on doping MgB_2 with graphene. Whereas Sudesh *et al.*(2013) have reported no change in T_c on doping of MgB_2 with graphene up to 10 wt%, Li *et al.*(2017) observed that T_c of MgB_2 monotonically decreases with increasing graphene content. This anomaly needs to be resolved by further experimental work in this regard.

Gonnelli *et al.* (2006) have used point contact spectroscopy to study the superconducting gaps in Al- and C-substituted MgB_2 single crystals. They observed that while phase segregation is important in $Mg_{1-x}Al_xB_2$ system at $x \geq 0.09$, in $Mg(B_{1-y}C_y)_2$ system a doping-induced transition takes place from two gaps to single gap superconductivity at $y \approx 0.132$.

To study effect of hole-doping on superconducting properties of MgB_2, Ahn *et al.* (2002) investigated structural and superconducting state properties of $MgB_{2-x}Be_x$ and observed that MgB_2 structure is maintained up to $x \approx 0.6$. The in-plane lattice constants (a and b) were found to decrease with increase in x, while the inter-plane lattice constant (c) was reported by them to increase with x. They also observed that whereas the superconducting transition temperature T_c of Be doped MgB_2 decreases monotonically with x, ΔT_c shows a maxima at $x \approx 0.3$. They further observed that the change in T_c can be correlated with the in-plane contraction of the lattice, which is consistent with 2D nature of σ-bands.

Xiyu *et al.* (2009) have investigated theoretically the Be and C co-doped MgB_2 system. They observed that on co-doping of MgB_2 by electrons and holes, the compensation effect is clearly visible from the band structure and Density of States (DOS) diagrams of the system. For the co-doped system, the DOS and T_c values were found by them to lie in between the relevant values for Be-doped and C-doped systems, T_c value of co-doped system being almost equal to that of un-doped MgB_2. They observed that for Be-doping, the total density of states at Fermi level is larger than that of MgB_2, which should give rise to T_c values higher than that of MgB_2. However, experimentally T_c values for this system are found to be lower than that of MgB_2. This indicates a research gap in the theory and needs further clarification.

In the present work the effect of electron/hole doping on electronic structure of MgB_2 has been re-investigated, particularly for changes in the valence band in Γ - A direction and the position of Dirac point like structure at K point with respect to the Fermi level on the band structure diagram, on increasing the level of electron/hole doping in it. In the present theory both these parameters are considered to be very critical for transformation of the system into superconducting phase. The density of states at Fermi level is another important parameter for the observed superconductivity in MgB_2, which is investigated in the present work for different levels of electron/hole doping in MgB_2. The electron/hole doping of MgB_2 is achieved by way of substitution of Boron by Carbon/Beryllium. In the above perspective, an attempt is made to investigate whether the changes in the band structure and density of states on increasing the

doping level, are indicative of changes in T_c, as revealed by experimental findings due to Takenobu *et al.* (2001) and Avdeev *et al.* (2003) for electron doping and Ahn *et al.* (2002) for hole doping. Electron density distribution also throws light on the electronic properties of different types of atoms in a system. As such, the effect of electron/hole doping on the electron density distribution of MgB_2 is also investigated in the present work, where for the sake of simplicity the investigations are restricted to (1,0,0) plane.

Method and Computational Details

In the present study we take for lattice parameters of MgB_2, a = b = 3.084Å and c = 3.523Å along with $\alpha = \beta = 90^o$ and $\gamma = 120^o$, as the input parameters (Lorentz *et al.*, 2001). These parameters were found to be justified as they satisfy the minimum energy requirement for MgB_2 primitive cell, as obtained from Energy-Volume diagram for a volume of 196.2952 au^3, which is in agreement with the cell volume of 195.8252 au^3, obtained from the above mentioned parameters. MgB_2 is a layered structure, for which the space group is 191(P6/mmm). The positions of Mg and two B atoms in the unit primitive cell were taken as (0, 0, 0), (1/3, 2/3, 1/2) and (2/3, 1/3, 1/2). WIEN2k software due to Blaha *et al.* (2001) is used for computation of electronic structure properties of MgB_2, which is based on the Density Functional Theory (DFT) (Hohenberg and Kohn, 1964). The functioning of this code is based on an iterative solution of Kohn Sham equations (Kohn and Sham, 1965), by using DFT in a plane wave set with projector-augmented wave pseudo potentials. The Perdew-Burke-Ernzerhof (PBE) potential functional (Perdew *et al.*, 1996A), which has been widely used in DFT calculations and has been found to appropriately account for the electron-ion and exchange-correlation (XC) interactions in materials with metallic components and in particular the systems with AlB_2 structure (Goyal *et al.*, 2012), is used in the present work. In PBE potential, the effects of exchange and correlation interaction are incorporated in the theory by using Generalized Gradient Approximation (GGA) due to Perdew *et al.* (1996B), which is theoretically more sound than other such methods, viz., the one based on Local Density Approximation (LDA) and provides better estimates of the material properties, like binding energy, lattice parameters etc., as observed by Fuchs *et al.* (1998).

A super cell of dimensions (2x2x1) was constructed for the electron / hole doping of MgB_2, which contains 4 Mg and 8 B atoms (in 4 pairs), out of which one of the pairs of the B atoms is replaced by carbon / beryllium atoms so that a doping level of 25% is achieved. Similarly, on replacing 2 pairs of B-atoms by C / Be atoms, the doping

level of carbon / beryllium in MgB_2 becomes 50%. Each structure is investigated for its band structure, density of states and electron density distribution by using WIEN2K. In the present investigations, $RMT \times K_{max}$ is taken = 7.0, and the number of K-points for lattice sums is taken as 1000. For checking convergence of sums, the minimum resolution for energy is taken = 0.0001eV, and for the charge convergence the minimum resolution is set = 0.001au.

Symmetry plays an important role in computational science, by virtue of which the requirement of summing on whole Brillöuin Zone is reduced to summing over only on a wedge of it. It is found that the symmetry of space group 191(P6/mmm) for MgB_2 is reduced to that of 65(C/mmm) group in carbon / beryllium doped MgB_2, for doping level of 25%, so as to satisfy the minimum energy requirements. From similar considerations, the space symmetry group for doping level of 50% of C/Be in MgB_2 was found to be 51(P/mma).

Results and Discussion

In the present work, the effect of electron/hole doping on band structure and density of states of MgB_2 has been investigated by substitution of carbon and beryllium atoms at B-sites. For electron / hole doping of MgB_2 at B-sites, C and Be are the natural choices, as they lie adjacent to B in the Periodic Table. The level of doping in the present investigations was kept 25% and 50% for both the impurities. The 2D projections of the primitive unit cell of MgB_2 and super cells of the structures $MgB_{1.5}C_{0.5}$, $MgB_{1.5}Be_{0.5}$, MgBC and MgBBe in (1,0,0) plane are shown in Figures 1(a) to 1(e) respectively, along with the electron density contours for these structures, as projected in the (1,0,0) plane for the sake of simplicity. It is apparent from these diagrams that although the cell structures of $MgB_{1.5}C_{0.5}$ and $MgB_{1.5}Be_{0.5}$ crystals shown in Figures 1(b) and 1(c) are identical, they differ in the sense that in the former C-atoms do not show bonding with B-atoms, whereas in the latter Be-atoms form bonds with B-atoms. The latter is in accordance with the fact that in Be-doped MgB_2, a fraction of electrons donated by Mg atoms fill up holes on Be atoms, undergoing sp3 bonding with B atoms. The core size of Be atoms is also very nearly equal to that of B-atoms, it being slightly larger than that of B-atoms, which creates favourable environment for formation of covalent bonds of B and Be atoms. On the other hand, the core size of C-atoms is somewhat less than that of B-atoms. This gives rise to lattice distortion near C-sites. As a result of it, C-atoms have lesser tendency to undergo covalent bonding with B-atoms. The unit cells for the case of 50% doping of C/Be atoms in MgB_2 at B-sites (shown in Figures 1(d) and 1(e)) are much simpler as compared to the relevant MgB_2 cells with 25% doping of C/Be. This is

because the symmetry involved in this case is comparatively higher than that of 25% doping. In this case, the two adjacent Mg atoms are so closely packed that they touch each other.

As apparent from Fig. 1(a), in pure MgB_2 the electron density contours are in the form of circular arcs centred at Mg atoms. The circular arcs are obtained without any deformation till they touch B-atoms. However, for 25% C-doping of MgB_2, i.e. for $MgB_{1.5}C_{0.5}$, the contours are obtained in the form of deformed circles or circular arcs around Mg
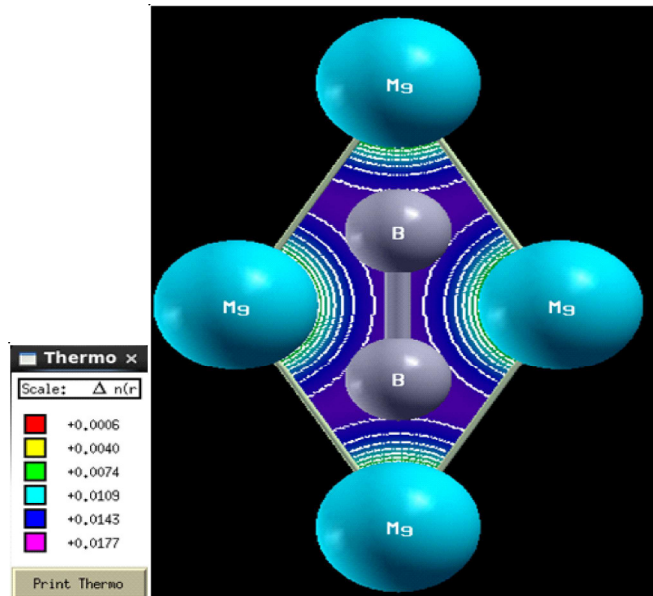
Fig. 1(a). Unit Cell & Electron Density for MgB_2
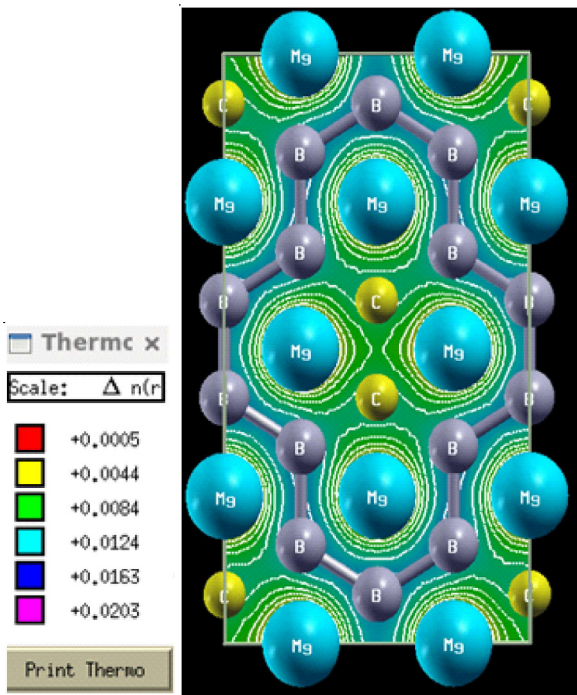
Fig. 1(b). Unit Cell & Electron Density for $MgB_{1.5}C_{0.5}$
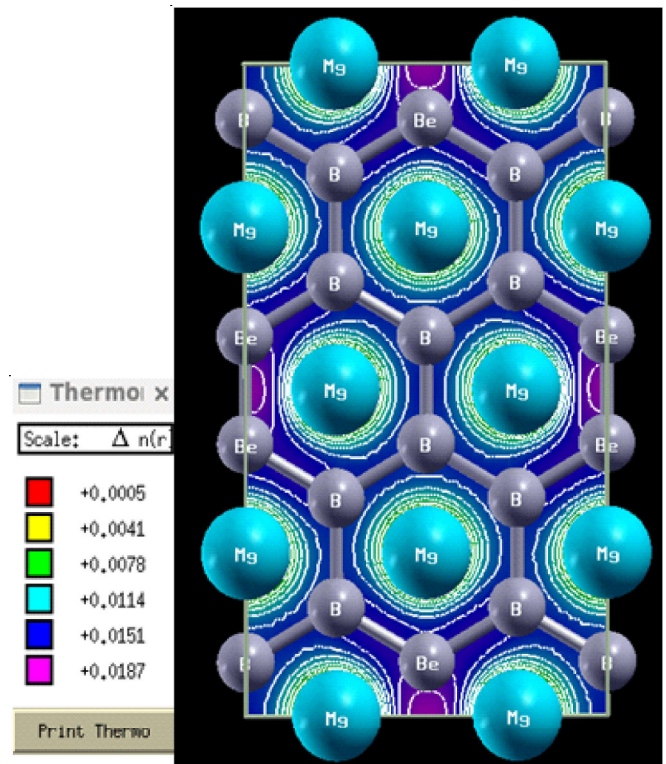
Fig. 1(c). Unit Cell & Electron Density for $MgB_{1.5}Be_{0.5}$

atoms, bulging out towards C-atoms. For the centrally placed Mg atoms, the deformed circles point towards the centre of the line joining the centrally placed C-atoms and the outer circular arcs of the two Mg atoms join together through carbon atoms to form a closed loop, as shown in Fig. 1(b). On the other hand, for 25% doping of MgB_2 by Be, i.e. for $MgB_{1.5}Be_{0.5}$, the deformation of circular contours around Mg atoms is found to be comparatively less. For centrally placed Mg atoms, the deformed circles are compressed from the side of Be atoms, so that they are densely populated on that side. On the other side, the contours are rarely populated towards B-atoms. The electron density contours also connect the nearby Be atoms with each other, as shown in Fig. 1(c). The difference in the behaviour of C-doped and Be-doped MgB_2 may be understood as follows: when C-atoms are substituted in MgB_2 crystal, they undergo sp3 bonding with B-atoms and reside in the B-layer. An extra electron on C-atom is contributed by it to the π band, which makes the interlayer bonding stronger. After donating an electron, C-atom behaves as if carrying +ve charge and attracts electrons. On the other hand, Be atom is short of one electron to form sp3 bonding, which it takes from the electrons residing on the boron sheet or π band, on being donated by the Mg atoms. The Be atoms, therefore, behave as if carrying –ve charge and repeal electrons.

In case of 50% doping of MgB_2 by C/Be atoms, it is observed that the electron density contours are quite different from the case of 25% doping of MgB_2. Now for C-doping, the contours are in the form of curves going around C-B bond, on both the sides of the bond. These curves are more curved in the vicinity of the C and B atoms and become less curved and less dense as we approach Mg atoms, as shown in Fig. 1(d) for MgBC Closed loops encircling C and B atoms are also obtained in this case. This shows that in the symmetry 51(P/mma), the extra electrons of C-atoms after they form sp3 bonds with B-atoms, are shared equally by C and B atomic sites, so that the electron density contours are symmetric around the two types of atoms. The outer curves converge on Mg atoms, showing that the electrons are attracted by Mg atoms. This is because in MgBC, Mg atoms acquire +ve charge after donating two electrons to the B-C layer and form ionic bonds. In case of Be-doping, the contours form closed loops in between Be and B atoms and also on the two sides of these atoms, showing that after undergoing sp3 hybridization, Be and B atoms acquire opposite polarity, which gives rise to closed e-contours. The opposite polarity on Be and B atoms may be on account of a hole present on Be-atom when it undergoes sp3 hybridization in the B-lattice and sharing of electrons donated by Mg atoms by different sites on B-layer, so that Be and B sites effectively acquire +ve and –ve charges respectively. Away from Be-B bond, the e-contours are almost straight lines as we approach Mg atoms, as shown in Fig. 1(e) for MgBBe. These lines also converse on Mg atoms, showing that they carry +ve charge and form ionic bonds.
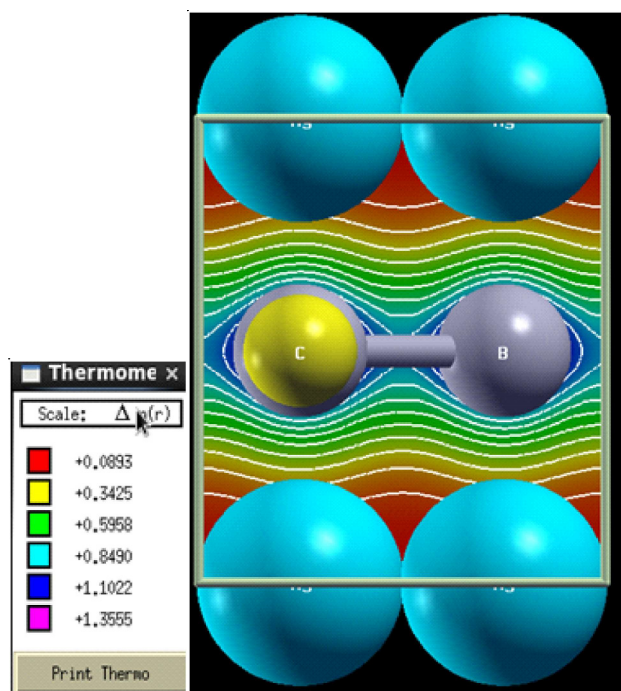

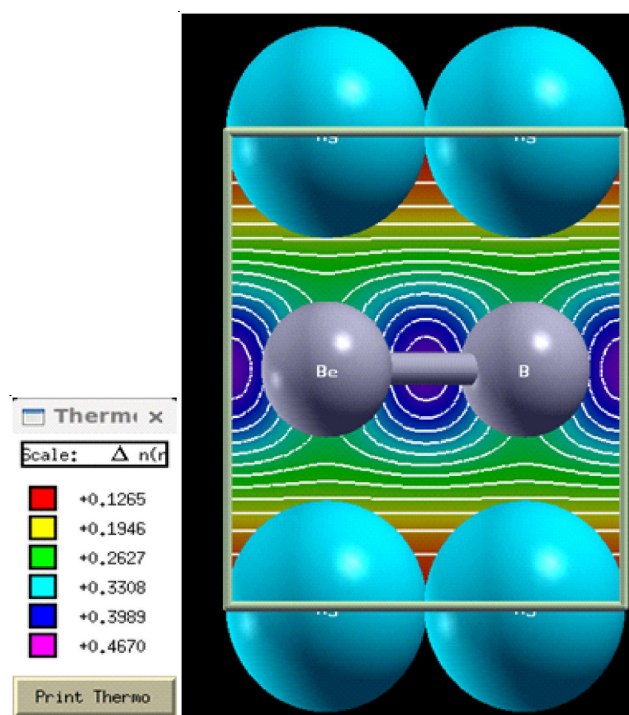**Fig. 1(e). Unit Cell & Electron Density for MgBBe**

Fig. 1(d). Unit Cell & Electron Density for MgBC

The band structure diagrams for MgB_2, $MgB_{1.5}C_{0.5}$, $MgB_{1.5}Be_{0.5}$, MgBC and MgBBe are shown in Figures 2(a) to 2(e), whereas the relevant Density of States (DOS) diagrams of these materials are given in Figures 3(a) to 3(e). Fig. 2(a) shows band structure for MgB_2, from where it is seen that in this case a Dirac point like structure is obtained at symmetry point K at 1.81 eV above the Fermi level. Also a doubly degenerate valence band in the Γ-A direction is in the form of a straight line with positive slope lying above the Fermi level, above 0.43 eV at Γ point and above 0.86 eV at A point, so that hole filling in this band in the states lying above the Fermi level becomes possible (The point Γ in Fig. 2(a) and other diagrams of Fig. 2 is represented by G). Hole filling in the valence band can also take place at symmetry point K, where the band projects 1.81 eV above the Fermi level. The valence band also projects just above the Fermi level at symmetry point M. On the other hand, the conduction band projects below the Fermi level at symmetry point L, where it can be filled up with electrons, favouring pair formation. The above mentioned features obtained in the band structure of MgB_2, are inline with the observations made by An and Pickett (2001), Liu *et al.* (2001), Mater (2008) and Kortus *et al.* (2005), according to which the filling of holes in σ bands, coupling of σ - bands to the optical phonons of B-lattice and bond stretching due to E_{2g} phonon modes may be considered responsible for lifting of degeneracy of $p_{x,y}$ bands along Γ- A direction, opening of band gaps, phase
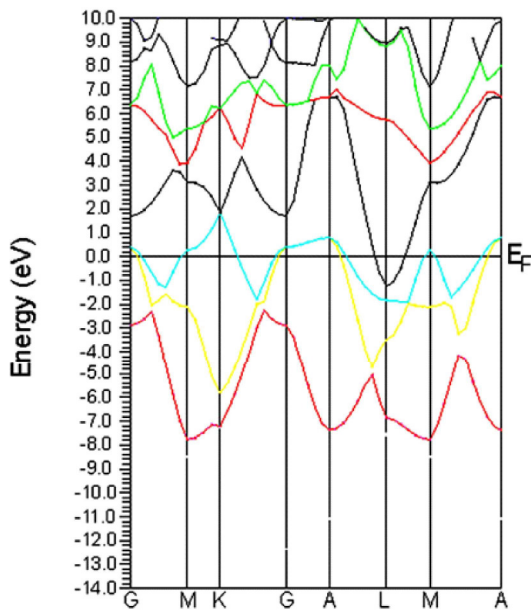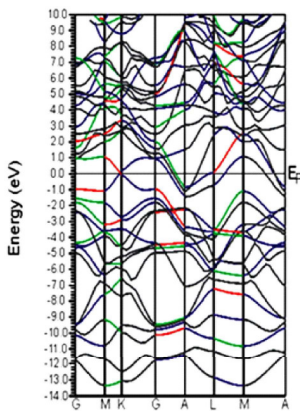
Fig. 2(a). Band Structure for MgB$_2$
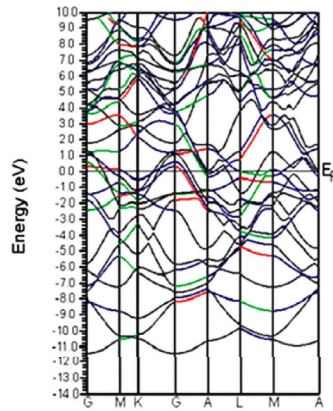

Fig. 2(b). Band Structure for MgB$_{1.5}$C$_{0.5}$

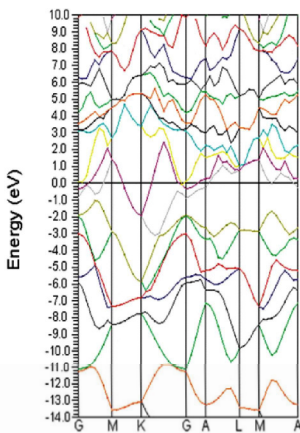**Fig. 2 (c). Band Structure for MgB$_{1.5}$Be$_{0.5}$**

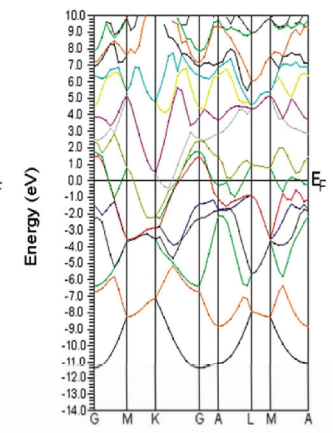**Fig. 2(d). Band Structure for MgBC**

Fig 2(e). Band Structure for MgBBe

transformation to the superconducting state and creating conditions for higher T$_c$ in this material. Further, It may be observed from Fig. 3(a), showing DOS of MgB$_2$, that the total DOS at Fermi level in this material is $\approx$ 0.71 states/eV, which along with the band structure features mentioned as above, forms appropriate conditions for MgB$_2$ to become superconductor at temperatures of the order of T$_c$ $\approx$ 40 K. It is also apparent from Fig. 3(a) that the major contribution to DOS at Fermi level comes from B-atoms, which shows that the layered honeycomb type structure of B-atoms plays a major role in superconducting behaviour of MgB$_2$. The important peaks in the DOS curve for MgB$_2$ on the two sides of Fermi level lie at -8.46, -2.19, +6.30 and +8.22 eV with peak heights of 0.58, 1.33, 1.73 and 1.44 states/eV respectively, which may correspond to different energy bands of MgB$_2$, shown in Fig. 2(a).
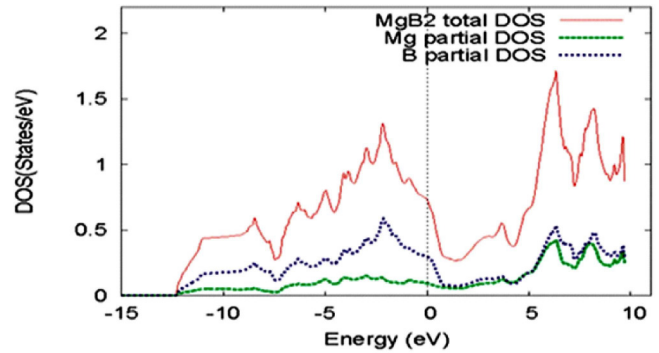

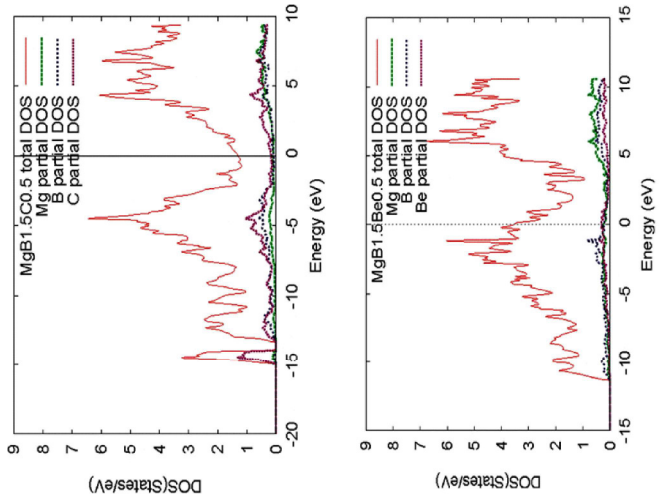**Fig. 3(a). Density of States for MgB$_2$**

Fig. 3(b). Density of States for MgB$_{1.5}$C$_{0.5}$

Fig. 3(c). Density of States for MgB$_{1.5}$Be$_{0.5}$

For 25% doping of MgB$_2$ with C, the relevant band structure diagram is shown in Figure 2(b). It is clear from this figure that the Fermi level goes up as a result of C-doping, so that the degenerate valence band in Γ-A direction falls below the Fermi level and becomes full with electrons. Consequently, there is no possibility of hole filling in this region of the valence band for MgB$_{1.5}$C$_{0.5}$.
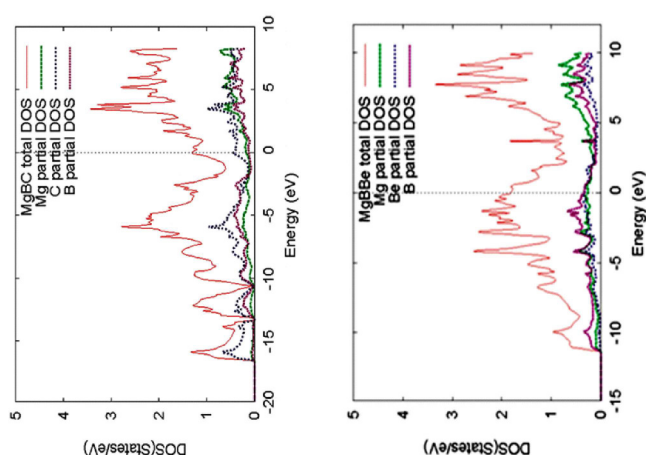
Fig. 3(d). Density of States for MgBC

Fig 3(e). Density of States for MgBBe

The shape of this band also changes in other regions of Brillöuin zone, as compared to that of MgB_2. It may also be observed from this diagram that the Dirac point like structure is now obtained on the Fermi level at symmetry point K, but the lines forming this point acquire curvature, so that the electrons no more behave as mass less particles. As a result of carbon doping, the band gap at Γ point increases from 1.4 eV to about 2.0 eV and since the lower band is almost full, favourable conditions for superconductivity do not exist. As a result of it, T_c decreases appreciably for this material. This is in agreement with the experimental findings for dependence of T_c on C-content in MgB_2, plotted by Kortus *et al.* (2005). On the basis of two band model for MgB_2, they observed that in case of e-doping of MgB_2, while band filling will decrease both the superconducting gaps, the interband scattering due to impurity atoms in B-plane will decrease the width of the larger gap and increase the width of the smaller gap. The two effects may compensate for the smaller gap, so that the this gap is nearly constant. On the other hand, they add up for the larger gap, so that the width of the that gap decreases. For small doping concentration, they considered the small k_z dispersion of σ bands along Γ- A line to be responsible for decrease in T_c. For enhanced doping level, experiments conducted on C-doped single crystals, indicate merging of the two superconducting gaps, which may be considered to be the manifestation of interband scattering. From Fig. 3(b) for Density of States, it is found that in $MgB_{1.5}C_{0.5}$ the DOS at Fermi level is about 1.14 states/eV. Although the DOS at Fermi level is increased as compared to the case of MgB_2, the valence band in Γ- A direction now lies below the Fermi level and does not support hole filling in valence band. As such, the conditions in $MgB_{1.5}C_{0.5}$ are not as favourable for superconducting transition, as in MgB_2. As such, this material becomes superconducting at lower values of T_c as compared to MgB_2. The important DOS peaks in this case, situated on the two sides of Fermi level,

are obtained at -14.26, -4.47, +4.26 and +6.81 eV, with peak heights of 3.17, 6.42, 6.00 and 5.92 states/eV respectively.

The energy band diagram for the case of 25% doping of MgB_2 with Be, is given in Fig. 2(c). The relevant DOS curves for this case are displayed in Fig. 3(c). It may be observed from Fig. 2(c) that as a result of Be-doping, the Fermi level goes down, so that the valence band in MgB_2 now goes up and the flat band in Γ- A direction lies above the Fermi level, the relevant energy values being +1.2 eV at Γ point and +1.6 eV at A point. Now, other lower lying band of MgB_2 serves as the valence band for this material. The shape of this band in Γ- A direction is found to be quite different from that of MgB_2. It is in the form of a straight line with –ve slope, which crosses the Fermi level, the energy values being about +1.2 eV at Γ point and -1.8 eV at A point. The lines forming Dirac point like structure at symmetry point K become curved and it is shifted to a position about 2.4 eV above the Fermi level. The value of DOS at Fermi level in this material is found to be 3.57 states/eV (Fig. 3(c)), but since the conditions of filling of valence band with holes in Γ- A direction and existence of a Dirac point like structure at symmetry point K are not satisfied, the conditions are not as favourable in this material as in MgB_2 for superconducting phase transition to occur. As such, T_c value for this material cannot be as high as in MgB_2. This is in consonance with the experimental observations made by Ahn *et al.*(2002) and provides a theoretical basis for decrease in T_c on hole-doping of MgB_2. This also provides a solution to the contradiction between the experimental findings of Ahn *et al.* (2002) and theoretical predictions made by Medvedeva *et al.*(2001) and Xiyu *et al.* (2009) for increase in T_c on doping MgB_2 with Be. The prominent DOS peaks obtained in this case on two sides of Fermi level lie at -2.22, -0.80, +6.00, +6.84, +8.09 and +9.38 eV, with peak heights of 5.17, 5.89, 6.70, 6.25, 6.07 and 5.71 states/eV respectively.

For 50% doping of C in MgB_2 (Fig. 2(d)), it is observed that the Fermi level further goes up, so that the valence band of MgB_2 further goes down below the Fermi level and the degeneracy of the flat band in MgB_2 in Γ- A direction is now lifted up. The flat bands in Γ-A region are now obtained slightly shifted towards the symmetry point K and lie in the energy range -5.4 eV to - 6.0 eV. Another band lying above the Fermi level in MgB_2, now passes through the Fermi level and behaves as the valence band. This band crosses the Fermi level in Γ-A region, with $E < E_F$ at Γ point and $E > E_F$ at A point. This band is also like a pair of two parallel bands, the position of the lower band being below the Fermi level. This band supports hole filling along A-L, L-M and M-A directions, but hole filling in Γ- A direction can be possible to a very little

extent. However, the Dirac point like structure at K point is now completely absent, which suggests that conditions favourable to superconductivity are not present in this material (MgBC). Fig. 3(d) reveals that DOS at Fermi level for this material is 1.30 states/eV, which along with hole filling tendency of valence band, as discussed above, make conditions favourable for superconductivity, but absence of Dirac point like structure at symmetry point K and rare possibility of hole filling in Γ- A direction reveal that on the whole favourable conditions for superconductivity do not exist in this material. This is in agreement with the observations made by Slusky *et al.* (2001) that for electron doping of 25% or more a non-superconducting phase is restored. The important DOS peaks on the two sides of the Fermi level in this case lie at -15.86, -12.00, -6.00, +3.43, +3.86 and +7.93 eV, with peak heights of 1.30, 1.30, 2.77, 3.42, 3.26 and 2.61 states/eV, respectively. Thus, on the whole, the conditions favourable for superconducting state do not exist in MgBC.

On the other hand for 50% doping of Be in MgB_2, it is observed from Fig. 2(e) that the Fermi level now further goes down, so that the valence band of MgB_2 is further shifted above the Fermi level. The shape of the doubly degenerate flat band of MgB_2 along Γ- A direction also gets distorted. Now the twin bands in Γ- A region touch only at a point at about 2.6 eV above the Fermi level. Another lower lying band of MgB_2, which now passes through the Fermi level, behaves as the valence band. This band crosses the Fermi level in Γ-A region, with $E > E_F$ at Γ point and $E < E_F$ at A point. Another similarly placed band also crosses the Fermi level in Γ- A region, with $E > E_F$ at Γ point and $E < E_F$ at A point. The Dirac point like structure observed in MgB_2 at symmetry point K is now completely absent, showing that favourable conditions for this material (MgBBe) to become superconductor do not exist. The hole filling in these bands becomes possible in Γ- A region as well as along L-M direction and at symmetry points Γ and M. The conduction band in this material also projects below the Fermi level near the K point. The electronic transition may, therefore, take place from the valence band to the conduction band. This may facilitate pairing of electrons. As such, limited chances exist for this material to become superconductor. MgBeB, therefore, becomes superconducting at T_c values lower than MgB_2. From Fig. 3(e), it can be observed that DOS at Fermi level is 1.89 states/eV, which also supports superconducting phase transition of this material. The important DOS peaks on this curve on the two sides of Fermi level lie at -10.07, -4.18 -2.80, -1.34, +3.73 and +7.84 eV, with respective DOS values of 0.95, 2.58, 2.47, 2.26, 1.89 and 3.37 states/eV. Higher values of DOS at Fermi level, chances of hole filling in Γ- A region and transition

of electrons from valence band to conduction band make this material more suitable for becoming a superconductor, as compared to C-doped MgB_2. This suggests that Be-doped MgB_2 stands better chances than C-doped MgB_2 to become a superconductor.

Conclusion

From the above analysis, it may be inferred that DOS at Fermi level is not the only deciding factor for a material to become superconductor. The hole filling in valence band in Γ-A direction, the appearance of Dirac point like structure at symmetry point K in the vicinity of the Fermi level, and presence of large amplitude high frequency phonon modes causing bond stretching and anharmonicity and their coupling with the in-plane σ bands of boron lattice are those important parameters which decide the occurrence of superconductivity and transition temperature (T_c) in the MgB_2 based materials. However, for moderate values of T_c, DOS at Fermi level should have substantial value, say of the order of 0.7 states/eV or more.

As all these conditions are fulfilled in MgB_2 it shows superconductivity at about 40K. In the absence of any of these characteristic properties, the superconducting phase either does not exist or occurs at lower values of T_c. On doping MgB_2 with carbon or beryllium, the delicate equilibrium of above mentioned conditions is disturbed. Therefore, T_c decreases as we increase the electron/ hole doping level in them and beyond a certain level of doping the material may no more show superconducting transition. It is learnt that at a particular level of doping, Be-doped MgB_2 stands better chances to become superconductor as compared to the C-doped MgB_2. A careful analysis of electronic structure of MgB_2 and related materials can, therefore, be of great help in predicting their transition to superconducting phase.

Acknowledgments

IISU

References

Ahn, J. S., Kim, Young-Jin, Kim, M. S., Lee, S. I., Choi, E. J. (2002) Structural and superconducting properties of $MgB_{2-x}Be_x$. *Phys Rev* **65**: 172503.

An J. M., Pickett, W. E. (2001) Superconductivity of MgB_2: Covalent bonds driven metallic. *Phys Rev Lett* **86**: 4366-4369.

Avdeev, M., Jorgensen, J. D., Ribeiro, R.A., Bud'ko, S. L., Canfield, P. C. (2003) Crystal chemistry of carbon-substituted MgB_2. *Physica* **C- Superconductivity** **387**: 301-306.

Bateni, A., Erdem, E., Repp., S., Acar, S., Kokal, I., Häßler, W., Weber, S., Somer, M. (2015) Electron paramagnetic resonance and Raman spectroscopy studies on carbon-doped MgB2 superconductor materials. *J Appl Phys* **117**: 153905(1-7).

Blaha, P., Schwarg, K., Madsen, G., Kvasnicka, D., Luitz, J. (2001) WIEN2K: An augmented plane wave plus local orbital program for calculating crystal properties. Kartheinz Schwartz, Techn. Universitat: Austria.

Cai, Q., Liu, Y., Ma, Z., Yu, L. (2014) Comparison of carbon-doped MgB_2 bulk fabricated from pre-synthesized Mg/CNT and Mg/amorphous carbon composites. *Appl Phys* **A114**: 919-924; doi: 10.1007/s00339-013-7764-6.

Choi, H. J., Roundy, D., Sun, H., Cohen M. L., Louie, S. G. (2002) The origin of the anomalous superconducting properties of MgB_2. *Nature Letters (London)* **418**: 758-760.

Dai, W., Ferrando, V., Pogrebnyakov, A. V., Wilke, R. H. T., Chen, Ke, Weng, X., Redwing, J., Bark, C. W., Eom, C. B., Zhu, Y., Voyles, P. M., Rickel, D., Betts, J. B., Mielke, C. H., Gurevich, A., Larbalestier, D. C., Li, Qi, Xi, X. X. (2011) High-field properties of carbon-doped MgB_2 thin films by hybrid physical-chemical vapour deposition using different carbon sources. *Supercond. Sci Technol* **24:** 125014(1-12); doi: 10.1088/0953-2048/24/12/125014.

De Silva, K. S. B., Xu, X., Li, W. X., Zhang, Y., Rindfleisch, M., Tomsic, M. (2011) Improving superconducting properties of MgB_2 by graphene doping. *IEEE Transactions on Applied Superconductivity* **21**: 2686-2689; doi: 10.1109/TASC.2010.2091938.

De Silva, K. S. B., Xu, X., Wang, X. L., Wexeler, D., Attard, D., Xiang, F., Dou, S. X. (2012) A significant improvement in the superconducting properties of MgB_2 by co-doping with graphene and nano-SiC. *Scripta Materialia* **67**: 802-805; doi: 10.1016/j.scriptamat.2012.07.014.

Fan, Y., Ru-Shan, H., Ning-Hua, T., Wei, G. (2002) Electronic structural properties and superconductivity of diborides in MgB_2 structure. *Chinese Phys Lett* **19**, 1336-1339; doi: 10.1088/0256-307x/19/9/337.

Fuchs, M., Bockstedte, M., Pehlke, E., scheffler, M. (1998) Pseudopotential study of binding properties of solids within generalized gradient approximation: The role of core-valence exchange correlation. *Phys Rev* **B57**: 2134-2145.

Gonnelli, R. S., Daghero, D., Ummarino, G. A., Calzolari, A., Dellarocca, V., Stepanov, V. A., Kazakov, S. M., Jun, J., Karpinski, J. (2006) A point-contact study of the superconducting gaps in Al-substituted and C-substituted MgB_2 single crystals. *J Phys Chem Solids* **67**: 360-364; doi: 10.1016/j.jpcs.2005.10.065.

Goyal, V., Sharma, R., Sharma, K.S. (2012) A theoretical investigation of superconductivity and electronic structure of AlB_2 and BeB_2. *International Journal of Advances in Science and Technology* **4** (May-Spl. Issue): 76-85; https://www.svpublishers.co.uk/#/ijast/4547363856.

Hohenberg, P., Kohn, W. (1964) Inhomogeneous electron gas. *Phys Rev* **136**: B864-B871; doi: 10.1103/PhysRev.136.B864.

Kazakov, S. M., Puzniak, R., Rogacki, K., Mironov, A. V., Zhigadlo, N. D., Jun, J., Soltmann, Ch., Batlogg B., Karpinski, J. (2005) Carbon substitution in MgB_2 single crystals: Structural and superconducting properties. *Phys Rev* **B71**: 024533(1-10).

Kim, J. H., Choi, S. (2015) Carbon doping induced imperfections in MgB2 superconducting wire. *Journal of Analytical Science and Technology* **6**: 11(1-5); doi: 10.1186/s40543-015-0048-3.

Kohn, W., Sham, L. J. (1965) Self-consistent equations including exchange and correlation effects. *Phys Rev* **140: A**1133-A1138.

Kong, Y., Dolgov, O. V., Jepson, O., Anderson, O. K. (2001) Electron-phonon interaction in normal and superconducting states of MgB_2. *Phys Rev* **B64**: 020501(1-5).

Kortus, J., Mazin, I. I., Belashchenko, K. D., Antropov, V. P., Boyer, L. L. (2001) Superconductivity of metallic boron in MgB_2. *Phys Rev Lett* **86**: 4656(1-4).

Kortus, J., Dolgov, O. V., Kremer, R. K.(2005) Band filling and inter-band scattering effects in MgB_2: Carbon versus Aluminium doping. *Phys Rev Lett* **94:** 027002(1-4).

Li, L., Zhang, H., Zhao, Y., Zhang, Y. (2017) Improved superconducting properties by graphene doping of

bulk MgB$_2$ prepared by the diffusion method. *IEEE Transactions on Applied Superconductivity* **PP(99)**: 1-4; doi: 10.1109/TASC.2017.2691584.

Lim, J. H., Lee, C. M., Park, J. H., Choi, J. H., Shim, J. H., Joo, J., Lee, Y. H., Kang W. N., Kim, C. J. (2009) Doping effect of CNT and nano-carbon in magnesium diboride bulk. *J Nanosci Nanotechnol* **9**: 7388-7392.

Liu, A. Y., Mazin, I. I., Kortus, J. (2001) Beyond Eliashberg superconductivity in MgB2.: anharmonicity, two phonon scattering and multiple gaps. *Phys Rev Lett* **87**: 087005 (1-4); doi: 10.1103/PhysRevLett.87.087.

Lorentz, B., Meng, R. L., Xue Y. Y., Chu, C. W. (2001) Thermoelectric power and transport properties of Mg$_{1-x}$Al$_x$B$_2$. *Phys Rev* **B64**: 052513; doi: 10.1103/PhysRevB.64.052513.

Lorentz, B., Meng, R. L., Chu, C. W. (2001) High pressure study on MgB$_2$. *Phys Rev* **B64**: 012507; doi: 10.1103/PhysRevB.64.012507.

Matar, S. F. (2008) Electronic structure and chemical bonding within MgB$_2$ and related borides from first principles. *Z. Naturforsch* **63b**: 673-680; *Verlag der Zietschrift für Naturforschung, Tübingen* 0932-0776/08/0600-0673$06.00 (c) 2008; http://znaturforsch.com.

Mc-Millan, W. L. (1968) Transition temperature of strong-coupled superconductors. *Phys Rev* **167**: 331-344.

Medvedeva, N. I., Ivanovskii, A. L., Medvedeva J. E., Freeman, A. J. (2001) Electronic structure of superconducting MgB2 and related binary and ternary borides. *Phys Rev* **B64**: 020502(1-4); doi: 10.1103/PhysRevB.64.020502

Mickelson, W., Cumings, J., Han W. Q., Zettl, A. (2002) Effect of carbon doping on superconductivity in magnesium diboride. *Phys Rev* **B65**: 052505(1-3).

Milman, V., Warren, M. C. (2001) Elastic properties of TiB$_2$ and MgB$_2$. *J Phys: Condens Matter* **13**: 5585-5595; doi: 10.1088/0953-8984/13/24/304.

Mudgel, M. Sharath Chandra, L. S., Ganesan, V., Bhalla, G. L., Kishan, H., Awana, V. P. S. (2009) Enhanced critical parameters of nano-carbon doped MgB2 superconductor. *J Appl Phys* **106**: 033904 (1-6).

Nagamatsu, J., Nakagawa, N., Muranaka, T., Zenitani, Y., Akimitsu, J. (2001) Superconductivity at 39K in magnesium diboride. *Nature Lett (London)* **410:** 63-64; doi: 10.1038/35065039.

Neaton J. B., Perali, A.(2001) On the possibility of superconductivity at higher temperatures in sp-valent diborides. *arXiv:cond-mat*/0104098v1 [cond-mat.supr-con] (pp. 1-27) 5 Apr. 2001.

Okatov, S. V., Ivanovskii, A. L., Medvedeva, Yu. E., Medvedeva, N. I. (2001) The electronic band structure of superconducting MgB$_2$ and related borides: CaB$_2$, MgB$_6$ and CaB$_6$. *Phys Stat Sol (b)* **225**: R3-R5.

Pena, O. de la, Aguayo, A., Coss, R. de (2002) Effect of Al doping on the structural and electronic properties of Mg$_{1-x}$Al$_x$B$_2$. *Phys Rev* **B66**: 012511; doi: 10.1103/PhysRevB.66.012511.

Perdew, J. P., Burke, K., Ernzerhof, M. (1996A) Generalized Gradient Approximation made simple. *Phys Rev Lett* **77:** 3865-3868; doi: 10.1103/PhysRevLett.77.3865; Erratum (1997): *Phys Rev Lett* **78**: 1396; doi: 10.1103/PhysRevLett.78.1396.

Perdew, J. P., Burke, K., Wang, Y. (1996B) Generalized Gradient Approximation for the exchange-correlation hole of a many electron system. *Phys Rev* **B54:** 16533-16539; Erratum (1998): *Phys Rev* **B57**: 14999; doi: 10.1103/PhysRevB.57.14999.

Ravindran, P., Vajeeston, P., Vidya, R., Kjekshus, A., Fjellvag, H. (2001) Detailed electronic structure studies on superconducting MgB$_2$. *Phys Rev* **B64**: 224509(1-15).

Ruiz-Chavarria, S.,Tavizon, G., Mora, de la P. (2006) Aluminium and carbon doped MgB2: band filling, band shift and anisotropy loss. *J Phys: Condens Matter* **18**: 1403-1412; doi: 10.1088/0953-8984/18/4/024.

Shah, M. C., Lone, A. G., Mir, I. A., Wani, T. A., Prasad, T. (2009) An SCDFT aspect of renormalized phonon-induced HTSC in doped HTSCD Mg$_{1-x}$Al$_x$B$_2$. *Oriental Journal of Computer Science & Technology* **2**: 177-180.

Shaikh, K., Shahabuddin, M., Ansari, I. A., Alzayed, N. S. (2013) Enhancement of superconducting properties of MgB$_2$ by doping of nano-Alumina and nano-carbon. *International Journal of Latest Research in Science and Technology* **2**: 55-58; http://www.mnkjournals.com/ijlrst.htm.

Sharma, G. (2016) Screening dependence of superconducting state parameters of carbon-doped MgB$_2$. *International Journal of Scientific & Engineering Research* **7**: 1056-1061; http://www.ijser.org.

Sharma, K. S., Bhargava, N., Jain, R., Goyal, V., Sharma, R., Sharma, S. (2010) Pseudo potential approach to superconductivity in MgB$_2$. *Indian J Pure & Appl Phys (NISCAIR)*. **48:** 59-66.

Sharma, R., Khan, S., Goyal, V., Sharma, V., Sharma, K.S. (2017) Investigation on effect of boron and nitrogen substitution on electronic structure of graphene. *Flatchem (Elsevier)* **1**: 20 -33; doi: 10.1016/j.flatc.2016.10.001.

Singh, Prabhakar P. (2003) Carbon doping in MgB_2:Role of boron and carbon $p_{x(y)}$ bands. *Solid State Commun* **127**: 271-274; doi: 10.1016/s0038-1098(03)00426-5.

Slusky, J. S., Rogado, N., Regan, K. A., Hayward, M. A., Khalifah, P., He, T., Inumaru, K., Loureiro, S. M., Haas, M. K., Zandbergen, H. W., Kava, R. J. (2001) Loss of superconductivity with the addition of Al to MgB_2 and a structural transition in $Mg_{1-x}Al_xB_2$. *Nature (London)* **410**: 343-345.

Sudesh, Kumar,N., Das, S., Bernhard, C., Varma, G. D. (2013) Effect of graphene oxide doping on superconducting properties of MgB_2. *Supercond Sci Technol* **26**: 095008(1-8); doi: 10.1088/0953-2048/26/9/095008.

Sun, Y., Yu, D., Liu, Z., Wang, T., He, J. Xiang, J., Zheng, D., Tian, Y. (2007) Structural and superconducting properties of Ca-doped MgB_2 superconductors. *Supercond Sci Technol* **20**: 261-266; doi: 10.1088/0953-2048/20/3/026.

Sunser, M. A., Bohnenstiehl, S. D., Dregia, S. A., Sumption, M. D., Yang, Y., Donovan, J. J., Collings, E. W. (2014) Homogeneous carbon doping of magnesium diboride by high-temperature, high-pressure synthesis. *Appl Phys Lett* **104**:162603; doi: 10.1063/1.4871578.

Takenobu, T., Ito, T., Chi, D. H., Prassides K., Iwasa, Y. (2001) Interlayer carbon substitution in MgB_2 superconductor. *Phys Rev* **B64:** 1345131(1-3).

Wu, L., Wan, B., Liu, H., Gou, H., Yao, Y., Li, Z., Zhang, J., Gao, F., Mao, Ho-kwang (2016) Co-existence of superconductivity and super-hardness in Beryllium Hexa-boride driven by inherent multicenter bonding. *J Phys Chem Lett* **7**: 4898-4904; doi: 10.1021/acs.jpclett.6b02444.

Xiyu, Su, Xiaoften, Zhi, Qinying, Hou, Wei, Cheng, Jiaxue, Liu (2009) First principles study of the Be-C co-doped MgB_2 system. *Journal of Semiconductors (Chinese Institute of Electronics)* **30**: 112001(1-5).

Yeoh, W. K., Zheng, R. K., Ringer, S. P., Li, W. X., Xu, X., Dou, S. X., Chen, S. K., MacManus-Driscoll, J. L. (2011) Evaluation of carbon incorporation and strain of doped MgB_2 superconductor by Raman Spectroscopy. *Scripta Materialia* **64**: 323-326; doi: 10.1016/j.scriptamat.2010.10.025.